Title
How Does Temporal Resolution Influence Geomagnetic Reversal Statistics?

Journal
Geophysical Research Letters, 46(10)

ISSN
0094-8276

Authors
Buffett, B
Avery, MS

Publication Date
2019-05-28

DOI
10.1029/2019gl082976

Peer reviewed

Geophysical Research Letters

RESEARCH LETTER
10.1029/2019GL082976

How Does Temporal Resolution Influence Geomagnetic Reversal Statistics?

B. Buffett[1] **and M. S. Avery**[1]

[1]Department of Earth and Planetary Science, University of California, Berkeley, CA, USA

Abstract Polarity intervals from marine magnetic anomalies exhibit variability that departs from a Poisson process. The deficit of short polarity intervals is well represented by a Weibull distribution with a shape parameter $k > 1$. Polarity intervals from a stochastic model also obey a Weibull distribution, but the shape parameter is controlled by the temporal averaging used to approximate the resolution of the marine record. Reducing the time averaging yields polarity intervals that are well described by a distribution with $k < 1$, suggesting that short polarity intervals are missing from the marine record. All of these missing polarity intervals are expected to occur when the dipole field is weak relative to the time average, often during transition states. We associate many of these short polarity intervals with frequent changes in the sign of the dipole during the transition. These short polarity intervals should be detectable in high-resolution observations of magnetic directions.

Key Points:
- Marine magnetic anomalies show a deficit of short polarity intervals relative to a Poisson process
- Stochastic models also predict fewer short polarity intervals when the temporal resolution is lowered to level of the marine record
- High-resolution records are expected to reveal more short polarity intervals than a Poisson process

Supporting Information:
- Supporting Information S1
- Data Set S1

Correspondence to:
B. Buffett,
bbuffett@berkeley.edu

Citation:
Buffett, B., & Avery, M. S. (2019). How does temporal resolution influence geomagnetic reversal statistics? *Geophysical Research Letters*, *46*. https://doi.org/10.1029/2019GL082976

Received 25 MAR 2019
Accepted 30 APR 2019
Accepted article online 2 MAY 2019

1. Introduction

Marine magnetic anomalies (MMA) over the past 160 Myr provide a detailed record of geomagnetic polarity transitions. The chronology of these transitions serves the basis of the geomagnetic polarity timescale (Ogg, 2012). All polarity intervals 30 kyr and longer are thought to be captured in the MMA record (Gee & Kent, 2015), although shorter, and previously unrecognized, polarity intervals are occasionally proposed (Krijgsman & Kent, 2004; Roberts & Lewin-Harris, 2000). Counter arguments usually invoke fluctuations in paleointensity to account for the anomalous paleomagnetic observations (Bowles et al., 2003; Lanci & Lowrie, 1997). Distinguishing between these two interpretations is important because it affects the statistics of geomagnetic reversals and our understanding of their physical origin.

An early investigation of the MMA record represented geomagnetic reversals as a Poisson process (Cox, 1969). The expected probability distribution for the polarity interval, τ, is governed by an exponential distribution, which requires the occurrence of short polarity intervals. A subsequent study (Naidu, 1971) favored a gamma distribution to account for the perceived deficit of short polarity intervals. The gamma distribution,

$$g(\tau) = \frac{\lambda^k}{\Gamma(k)} \tau^{k-1} e^{-\lambda \tau}, \tag{1}$$

is specified by two parameters; λ defines the rate of the process and k is a shape parameter that describes deviations from an exponential distribution. Here $\Gamma(k)$ is the gamma function. An exponential distribution is recovered by setting $k = 1$. Fewer short polarity intervals are expected when $k > 1$, whereas more short polarity intervals are predicted when $k < 1$ (see Figure 1). The current MMA record favors $k > 1$ (Lowrie & Kent, 2004; Naidu, 1971), and this result is supported by arguments about the finite time required for polarity transitions to occur (Merrill & McFadden, 1994). This line of reasoning is taken as evidence that geomagnetic reversals cannot be strictly a Poisson process.

Dynamo models have not yet clarified the most appropriate probability distribution for geomagnetic reversals. Even the most realistic simulations (e.g., Schaeffer et al., 2017) are still very far from Earth-like conditions, and these models are presently too computationally demanding to run for long enough to collect statistics on geomagnetic reversals. Instead, the numerical models must adopt very high values for fluid viscosity to allow long integrations and a sufficient sampling of polarity transitions (e.g., Driscoll & Olson, 2009). Such high viscosities restrict the fluid motions to large scales, so we might question whether these models are capable of producing short polarity intervals. The study of Driscoll and Olson (2009) reported no polarity intervals shorter than about two dipole diffusion times, which corresponds to

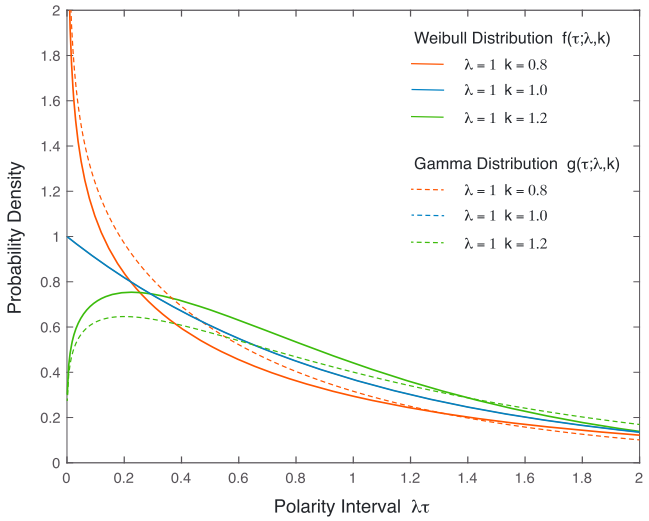

Figure 1. Gamma and Weibull probability density functions for the polarity interval, τ, scaled by the rate parameter λ. Both of these distributions specify the relative occurrence of short polarity intervals using a shape parameter k. More (less) short polarity intervals occur when $k < 1$ ($k > 1$). An exponential distribution ($k = 1$) describes the polarity intervals from a Poisson process.

roughly 100 kyr. Lhuiller et al. (2013) also reported long polarity intervals in dynamo simulations, although they were able to drew several interesting conclusions about the statistics of chron lengths. In particular, they found that the use of filtering to isolate polarity transitions in the simulations affected the shape parameter k.

Another approach relies on stochastic models for the paleomagnetic field (e.g., Brendel et al., 2007). These models have a physical basis (Scullard & Buffett, 2018), and they are capable of reproducing many observed properties of the paleomagnetic field (e.g., Buffett & Puranam, 2017; Meduri & Wicht, 2016). For this reason we use stochastic models to address the question of reversal statistics and to quantify the extent to which these statistics are affected by the temporal resolution of the geological record.

2. Stochastic Model for the Paleomagnetic Field

Fluctuations in the axial dipole moment, $x(t)$, can be represented conceptually by the motion of a particle in a double potential well (see Figure 2). The particle settles toward the base of one of the potential wells, but random noise continuously disturbs the motion. The source of noise is intended to reflect the influence of random convective fluctuations on the dipole moment. Occasionally, a series of random fluctuations push the particle across the barrier between the two potential wells, causing a polarity transition. The amplitude of the random noise and the general form of the potential well can be estimated from paleomagnetic observations. Here, we adopted the double potential well, $U(x)$, and the noise amplitude, $D(x)$, recovered by Buffett and Puranam (2017) from stacks of relative paleointensity measurements from the past 2 Myr (Ziegler et al., 2011), supplemented with higher-resolution measurements from the past 10 kyr (Constable et al., 2016). We treat the noise amplitude as a constant, which allows us to recover a representative estimate for D from the 10-kyr CALS10k2 model. The potential is based on the 2-Myr PADM2 M model using the functional form given in equation (27) from Buffett and Puranam (2017). Realizations of the stochastic model are computed by numerically integrating the stochastic differential equation

$$\mathrm{d}x = -\left(\frac{\partial U}{\partial x}\right)\mathrm{d}t + \sqrt{2D}\,\mathrm{d}W, \tag{2}$$

using an Euler-Maruyama method (Risken, 1989) with a discrete time step of $\Delta t = 1$ kyr. Here $\mathrm{d}W$ represents uncorrelated (white) noise drawn from a normal distribution with mean of 0 and variance of Δt.

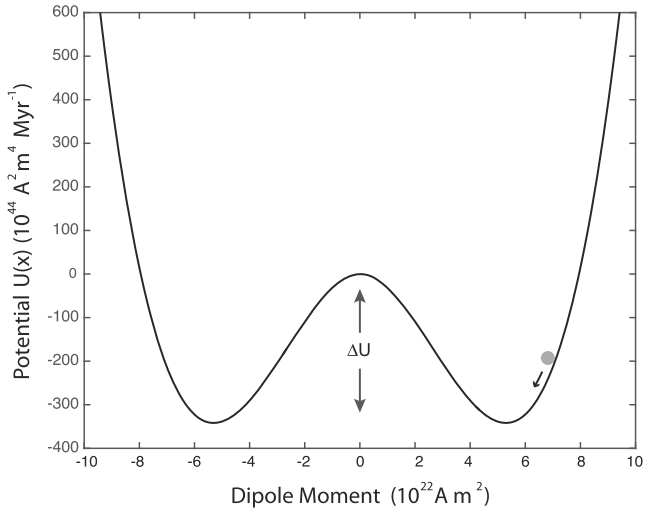

Figure 2. Motion of a particle in a double potential well, $U(x)$, is analogous to the stochastic model for the dipole moment. The particle settles toward the bottom of a potential well, but random noise continuously disturbs the state x. A sequence of disturbances can occasionally send the particle over the barrier at $x = 0$, causing a polarity transition.

We assess the statistics of polarity intervals using the mean, median, and standard deviation of τ recovered from realizations of the stochastic model. Dividing the median and standard deviation by the mean yields quantities that are independent of the rate, λ. This choice allows us to focus attention on the shape parameter k. We interpret the stochastic model using a Weibull distribution

$$f(\tau) = k\lambda^k \tau^{k-1} e^{-(\lambda\tau)^k}, \tag{3}$$

where λ and k are the rate and shape parameters (analogous to the parameters in the gamma distribution). The Weibull and gamma distributions are similar in many respects (see Figure 1), and they give nearly indistinguishable fits to the chron lengths from marine magnetic anomalies (see Figure S1). The main advantage of the Weibull distribution is the availability of a simple closed-form expression for the median. The normalized median is

$$\tilde{m} = \frac{(\ln 2)^{1/k}}{\Gamma(1+1/k)}, \tag{4}$$

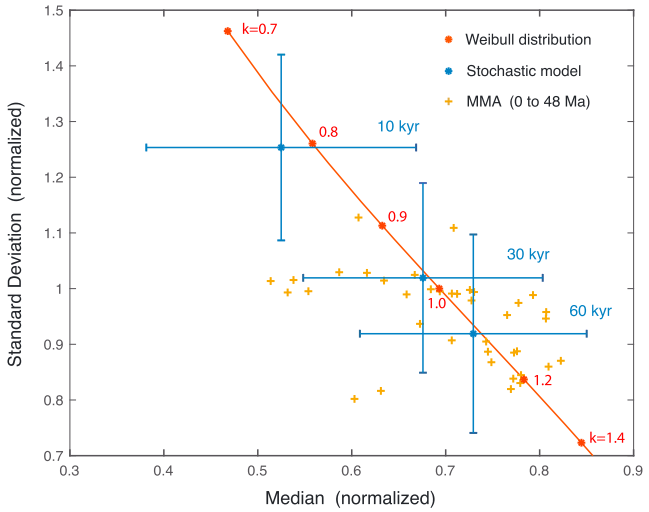

Figure 3. Normalized median, $\tilde{m}$, and standard deviation, $\tilde{\sigma}$, for a Weibull distribution (red). Statistics for the observed polarity intervals are computed from 10-Myr intervals of the marine magnetic anomaly record. The cloud of points is generated by shifting the 10-Myr interval back in time at increments of 1 Myr. Polarity intervals from the stochastic model follow a Weibull distribution, where the shape parameter, k, is set by the temporal resolution of the realization. The error bars represent the 1-sigma uncertainty from two hundred 10-Myr realizations.

and the normalized standard deviation is

$$\tilde{\sigma} = \left[\Gamma(1+2/k)/\Gamma(1+1/k)^2 - 1\right]^{1/2}. \quad (5)$$

Both of these expressions are independent of the rate parameter λ.

Variations in $\tilde{m}$ and $\tilde{\sigma}$ with k for the Weibull distribution are shown in Figure 3. Higher values of k yield lower $\tilde{\sigma}$ and higher $\tilde{m}$. Conversely, lower values of k give higher $\tilde{\sigma}$ and lower $\tilde{m}$. An exponential distribution ($k = 1$) has $\tilde{\sigma} = 1$ and $\tilde{m} = \ln 2$. Observations of the normalized median and standard deviation from the GPTS 2012 record (Ogg, 2012) are superimposed on the predictions for the Weibull distribution in Figure 3. Each point in Figure 3 is computed from the sample mean, median, and standard deviation in a single 10-Myr time interval. This interval is shifted back in time in increments of 1 Myr to produce a set of estimates that extend back to 48 Ma. The scatter of points falls on top of the Weibull distribution between $k = 0.9$ and 1.2, although the majority of points lie between $1 < k < 1.2$. This preference for $k > 1$ is consistent with a deficit of short polarity intervals.

We compare this result with the predictions of the stochastic model by running a series of 10-Myr realizations. We recover a single estimate for $\tilde{m}$ and $\tilde{\sigma}$ from each realization. Combining the results of 200 realizations gives a reliable sample mean and variance. Each realization is filtered in time using a running average to account for the limited temporal resolution of the geological observations. Distinct results for the reversal statistics are recovered with different choices for the averaging time. Calculations with an averaging time of 10, 30, and 60 kyr are shown in Figure 3, together with the 1-sigma error bars. The normalized median and standard deviation from the stochastic model follow the trend from the Weibull distribution, where the averaging time appears to correspond to a particular value of k. An averaging time of 10 kyr corresponds roughly to $k \approx 0.8$, whereas an averaging time of 60 kyr corresponds to $k \approx 1.1$. Interestingly, the stochastic model with a time average of 30 kyr has reversal statistics very close to the predictions for an exponential distribution ($k = 1$). Similar values for the shape parameter have been recovered from dynamo simulations using comparable levels of filtering (see Table 2 of Lhuiller et al., 2013).

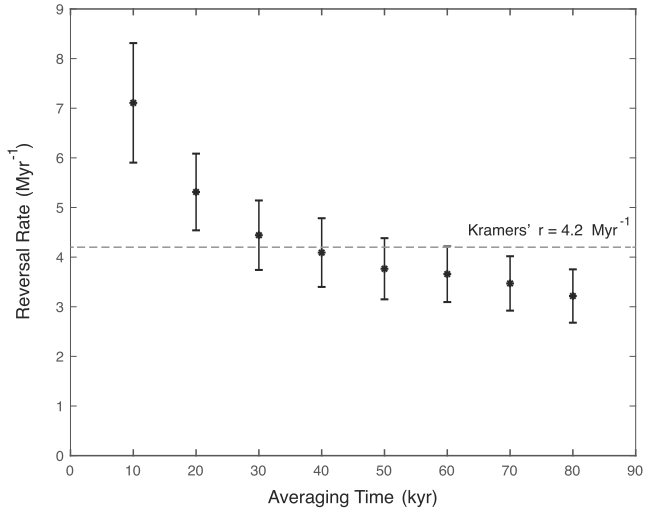

Figure 4. Average reversal rate, r, from two hundred 10-Myr realizations of the stochastic model. Changes in temporal averaging cause a systematic trend in r. An estimate of r from Kramers' formula (Risken, 1989) corresponds most closely to an averaging time of 30 to 40 kyr. A shorter averaging time causes a marked increase in r.

The correspondence between the predictions of the stochastic model and a Weibull distribution suggests that the shape parameter can be interpreted as a measure of the temporal resolution of record. We cannot strictly equate the averaging time to a temporal resolution because about 12% of the polarity intervals from the stochastic model are shorter than the averaging time. Still, we can expect the temporal resolution to be proportional to the averaging time. A longer averaging time yields a deficit of short polarity intervals relative to a Poisson process, so we might reasonably expect a low-resolution record to yield statistics with $k > 1$. This outcome is not entirely surprising, but we can now quantitatively assess how the statistics change when the temporal resolution is altered.

3. Consequences of Temporal Resolution

A large number of short polarity intervals are predicted by the stochastic model when the averaging time is low (e.g., $k < 1$), suggesting that the geological record is missing short polarity intervals. The direct influence of averaging time on the rate of polarity transitions is shown in Figure 4. We use a large ensemble of 10-Myr realizations to compute the mean reversal rate and its uncertainty. The error bars are mainly determined by the duration of the record; longer realizations produce smaller error bars. A 10-Myr realization is chosen to match our analysis of the observed

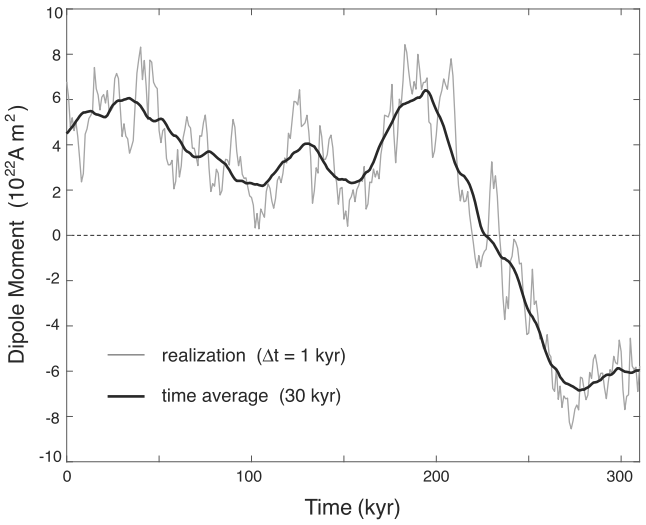

Figure 5. Realization of the stochastic model through a polarity transition. A smooth transition between stable polarities occurs when a time average of 30 kyr is applied to account for the temporal resolution of the marine magnetic anomaly record (black). The actual realization (gray) exhibits several zero crossings when the dipole moment is weak. Fluctuations in the dipole moment during the transition can reach $x = \pm 3 \times 10^{22}$ A/m^2.

polarity intervals. As we reduce the averaging time from 80 to 10 kyr, there is a steady increase in the rate of reversals. An estimate of the reversal rate from Kramers' formula (see equation (28) in Buffett & Puranam, 2017) is also shown in Figure 4. Kramers' formula can be interpreted as the mean time it takes for a particle at the bottom of one potential well to reach the top of the barrier. The slightest nudge sends this particle sliding down into the second potential well. The prediction of Kramers' formula agrees well with the outcome of model realizations when the averaging time is roughly 30 to 40 kyr. The reason for this correspondence is related to the typical duration of polarity transitions.

When a particle is placed at the top of the barrier, it will eventually make its way to the bottom of a potential well. We can use the stochastic model to predict how long this descent takes, at least on average. An estimate can be recovered from a large number of realizations, or the problem can be formulated in terms of a solution of the Fokker-Planck equation (Risken, 1989). In either case, we compute a recovery time of about 28 kyr (Buffett & Puranam, 2017), which is in good agreement with the average value inferred from the PADM2 M model of Ziegler et al. (2011). In other words, we can expect the dipole moment to return to its time-averaged amplitude roughly 28 kyr after a reversal. At this point the dipole begins its next attempt to cross the barrier from a position near the bottom of a potential well. More complicated trajectories are evident if we focus on the evolution of the dipole while it remains near the top of the barrier after a reversal. For example, a particle might return to the original polarity shortly after moving into the reversed polarity. Most of the details of these trajectories are suppressed by averaging over a timescale that is comparable to the recovery time (see Figure 5). We record only the dipole arriving at the bottom of a potential after roughly 30 kyr (on average). Starting the next reversal process from the bottom of a potential well is precisely the context that Kramers' formula was intended to approximate.

We now consider the more complicated trajectories that become possible when the temporal averaging is reduced. A relatively small fluctuation is sufficient to send the dipole back over the barrier when the time after a reversal is too short to allow the dipole to settle into a stable polarity. As we decrease the averaging time below the recovery time of 28 kyr, we begin to identify reversals in the stochastic model that occur before the amplitude of the dipole has fully recovered. Once the averaging time drops below 10 kyr, we have nearly doubled the rate of reversals, and all of these additional reversals occur when the geomagnetic field is weak relative to its long-term average. Detecting these reversals in the geological record would be difficult for two reasons. First, we need sufficient temporal resolution to identify short polarity transitions. Second, we need to detect short chrons when the amplitude of the dipole field is weak. Contributions from the nondipole part of the field become more important when the dipole is weak, so short polarity intervals are liable to have a complex geographic expression in paleomagnetic observations (Brown et al., 2007).

On strictly theoretical grounds we expect the reversal rate in the stochastic model to increase without limit as the averaging time decreases. This surprising outcome is actually consistent with the predictions of the Weibull distribution. To understand this behavior, we note that the stochastic differential equation in (2) describes a Wiener process near $x = 0$ because the gradient of the potential vanishes. If we discretize the solution by taking fixed time steps (say $\Delta t = 1$ kyr), then the number of times $x(t)$ crosses zero, on average, is proportional $\sqrt{n}$, where n is the number of 1-kyr time steps through the transition (DasGupta & Rubin, 1998). Here the transition duration is taken to mean the time needed for the dipole to settle into a stable polarity. Decreasing the time step improves the temporal resolution, but this change increases the number of time steps through the transition; it also increases the number of zero crossings. All of these additional zero crossings occur at the shortest time interval permitted by the refinement in the time step. In other words we are accumulating zero crossings with small τ, consistent with the expected correspondence between a small temporal resolution (Δt) and a small shape parameter $k < 1$. In the limit as Δt and k go to zero, the normalized median in (4) also goes to zero. This means that the polarity intervals cluster without limit near $\tau = 0$.

In practice, we cannot allow the time step in the stochastic model to decrease without limit because the noise term would no longer be uncorrelated. Numerical dynamo models (e.g., Buffett & Matsui, 2015; Olson et al., 2012) suggest that the correlation time of convective fluctuations is shorter than the overturn time, $L/V_{\mathrm{rms}} = 160$ years, where $L = 2,260$ km is the thickness of the outer core and $V_{\mathrm{rms}} = 0.45$ mm/s is an estimate of the convective velocity (Holme, 2015). We can think of the correlation time as a limit on the allowable temporal resolution for a standard stochastic model. Such a model could plausibly permit polarity intervals as short as a few hundred years if there were no other restrictions on our ability to record the dipole field. Of course, the amplitude of the dipole field between these transitions would be small, and such events would not conform to our usual view of geomagnetic reversals. However, there is no simple way to separate the continuum of behavior between low-amplitude and short-period polarity intervals and the more conventional view of geomagnetic reversals as a transition between two states of stable polarity. In fact, our conventional view may be partially shaped by the coincidence of dipole recovery time with the temporal resolution of the MMA record. Under these conditions, the dipole moves smoothly from one polarity to the other without much complexity during the transition.

4. Discussion

Several lines of evidence point to short polarity intervals in the paleomagnetic record. Confirmation of new polarity transitions in high-resolution sediment cores, like those proposed by Roberts and Lewin-Harris (2000), would shift the statistics of geomagnetic reversals toward lower values for k. Geomagnetic excursions are another type of brief event that sometimes exhibit directional changes of approximately 180° before returning to the direction established prior to the excursion (e.g., Laj et al., 2006). Laj and Channell (2015) prefer to describe these events as microchrons because their duration is less than 10 kyr. These events are too short to be detected in the MMA record, where the resolution for the fastest plate spreading rate is about 25 kyr (Gee et al., 1996). Including microchrons in the reversal statistics would shift the distribution to lower k. There are also indications of precursors and rebound features in magnetic directions around the time of well-established polarity transitions (Valet et al., 2012). Magnetic directions can change by 90° or more before and after the main transition. It is possible that some of these features represent short-period polarity transitions during times when the dipole is fluctuating about a weak state. It is common for the stochastic model to exhibit three or more sign changes during a transition from one stable state to another (see Figure 5). The main question is whether the amplitude of the dipole field between these sign changes is large enough to be detected in magnetic directions.

A weak dipole field allows magnetic directions to be strongly influenced by the nondipole field. These directions become increasingly aligned with the dipole when the strength of the dipole rises above the level of the nondipole field. The strength required to align magnetic directions with the dipole depends on the amplitude of nondipole components and on the geographic location of the observations (Quidelleur et al., 1999). The study of Brown et al. (2007) used the nondipole components from the CALS7k.2 model (Korte & Constable, 2005) to show that magnetic directions during a polarity transition cluster around the final direction once the dipole moment reaches $x = 2.5 \times 10^{22}$ A/m^2. Some geographic locations have magnetic directions aligned with the dipole when axial dipole moment is as small as $x = 2 \times 10^{22}$ A/m^2 (Brown & Korte, 2016; Valet & Plenier, 2008). We can use the time required for the dipole to reach to a suitable threshold to establish the duration of the shortest detectable chron in measurements of magnetic direction. An approximate expression for the average recovery time, τ_t, is (Buffett, 2015)

$$\tau_t = \frac{4x_t^2}{D\pi^2}, \tag{6}$$

where x_t is the prescribed threshold and D was previously defined as the amplitude of the noise term. This simple expression overestimates τ_t when the threshold is set at the time-averaged dipole moment (i.e., $x_t = 5.3 \times 10^2$ A/m^2). We obtain 33 kyr from (6) compared with 28 kyr from a full solution of the Fokker-Planck equation using $D = 0.34 \times 10^{44}$ A^2·m^4·kyr^{-1} (Buffett & Puranam, 2017). However, the discrepancy between (6) and a more extract treatment is substantially reduced when the threshold is lowered. For $x_t = 2.5 \times 10^{22}$ A/m^2, we obtain $\tau_t = 7.5$ kyr, which is comparable to values commonly cited for the duration of a reversal in magnetic direction (Clement, 2004). A duration predicted from (6) represents an ensemble average, so shorter (and longer) transitions are permitted. On the other hand, consistently shorter durations would imply a lower threshold for establishing a stable magnetic direction. For example, taking

$x_t = 2 \times 10^{22}$ A/m^2 gives an average duration of 4.8 kyr. Any specific instance of the stochastic process could plausibly give durations that were 50% higher or lower. This means that we might establish a new magnetic direction on timescales as short as 2.4 kyr if a dipole moment of $x_t = 2 \times 10^{22}$ A/m^2 was sufficient to define a stable magnetic direction.

Detectable polarity intervals with durations shorter than 10 kyr require fluctuations in the dipole about a weak state (nominally $x < 3 \times 10^{22}$ A/m^2). This behavior is distinct from suggestions of a correlation between reversal rate and field intensity (e.g., Tauxe, 2006) because the field intensity in this context is usually intended to represent the time average. Many of the short polarity intervals in the stochastic model occur when the field intensity is decreasing into a transition state. Several changes in polarity can occur before the magnetic field passes through the transition and reestablishes the time-averaged amplitude. The stochastic model offers a more complicated view of magnetic reversals because we find many short polarity intervals interspersed through a conventional reversal, based on the MMA record. Detecting these short events would require high-resolution sedimentary records, especially at time periods with tiny wiggles in the marine anomalies. A weak paleointensity (Bowles et al., 2003; Lanci & Lowrie, 1997) is precisely the condition needed to allow short polarity intervals.

5. Conclusions

A statistical analysis of the observed polarity intervals in the MMA record supports the view that geomagnetic reversals are not represented by a Poisson process. The observed record reveals a deficit of short polarity intervals relative to the predictions of a Poisson process. Instead, the observations are better represented by a Weibull probability density with a shape parameter $k > 1$. Polarity intervals from a stochastic model are also found to obey a Weibull distribution. However, the shape parameter is controlled by the temporal averaging applied to the stochastic model to represent the finite resolution of geological observations. Applying an averaging time of 30 kyr to the stochastic model yields a distribution of polarity intervals that closely follows a Poisson process. Adopting a lower time average, or equivalently using higher-resolution observations, gives polarity intervals that follow a Weibull distribution with a shape parameter $k < 1$. This result means that short polarity intervals are preferentially generated by the stochastic model relative to the predictions of a Poisson process. We suggest that these short polarity intervals are not captured in the MMA record, but they may be detected in paleomagnetic observations from high-resolution sediments core. Brief geomagnetic excursions that shift magnetic directions through 180° may be representative examples of this type of short event. All of these short events should occur when the dipole field is weak relative to the time average. Thus, we expect to find a weak dipole amplitude between closely spaced reversals in magnetic direction.

Acknowledgments
This work is partially supported by a grant (EAR-1644644) from the National Science Foundation to B. B. and by Posdoctoral Fellowship (EAR-1725798) from the National Science Foundation to M. S. A. We thank Andy Biggin and an anonymous reviewer for helpful comments and suggestions that improved this paper. Computer software used to generate the results in this paper are included in the supporting information.

References

Bowles, J., Tauxe, L., Gee, J., McMillan, D., & Cande, S. (2003). Source of tiny wiggles in Chron C5: A comparison of sedimentary relative intensity and marine magnetic anomalies. *Geochemistry, Geophysics, Geosystems*, *4*(6), 1049. https://doi.org/10.1029/2002GC000489

Brendel, K., Kuipers, J., Barkema, G. T., & Hoyng, P. (2007). An analysis of fluctuations of the geomagnetic dipole. *Physics of Earth and Planetary Interiors*, *162*, 249–255. https://doi.org/10.1016/j.pepi.2007.05.005

Brown, M. C., Holme, R., & Bargery, A. (2007). Exploring the influence of non-dipole field on magnetic records for field reversals and excursions. *Geophysical Journal International*, *168*, 541–555.

Brown, M. C., & Korte, M. (2016). A simple model for geomagnetic field excursions and inferences for paleomagnetic observations. *Physics of Earth and Planetary Interior*, *254*, 1–11.

Buffett, B. (2015). Dipole fluctuations and the duration of polarity transitions. *Geophysical Research Letters*, *42*, 7444–7451. https://doi.org/10.1002/2015GL065700

Buffett, B., & Matsui, H. (2015). A power spectrum for the geomagnetic dipole moment. *Earth and Planetary Science Letters*, *411*, 20–26. https://doi.org/10.1016/j.epsl.2014.11.045

Buffett, B., & Puranam, A. (2017). Constructing stochastic models for dipole fluctuations from paleomagnetic observations. *Physics of Earth Planetary Interiors*, *272*, 68–77.

Clement, B. M. (2004). Dependence of the duration of geomagnetic polarity reversals on site latitude. *Nature*, *428*, 637–640.

Constable, C., Korte, M., & Panovska, S. (2016). Persistent high paleosecular variations in the Southern Hemisphere for at least 10000 years. *Earth and Planetary Science Letters*, *453*, 78–86.

Driscoll, P., & Olson, P. (2009). Polarity reversals in geodynamo models with core evolution. *Earth and Planetary Science Letters*, *282*, 24–33. https://doi.org/10.1016/j.epsl.2009.02.017

Gee, J. S., & Kent, D. V. (2015). Sources of oceanic magnetic anomalies and the geomagnetic polarity timescale. In G. Schubert (Ed.), *Treatise on geophysics* (Vol. 5, 2nd ed., pp. 419–460). Amsterdam: Elsevier.

Gee, J. S., Schneider, D. A., & Kent, D. V. (1996). Marine magnetic anomalies as recorders of geomagnetic intensity variations. *Earth and Planetary Science Letters*, *144*, 327–335.

Holme, R. (2015). Large-scale flow in the core. In G. Schubert (Ed.), *Treatise on geophysics* (Vol. 8, 2nd ed., pp. 91–113). Amsterdam: Elsevier.

Korte, M., & Constable, C. G. (2005). Continuous geomagnetic field models for the past 7 millenia: 2, CALS7K. *Geochemistry, Geophysics, Geosystems*, *6*, Q02H16. https://doi.org/10.1029/2004GC000800

Krijgsman, W., & Kent, D. V. (2004). Non-uniform occurrence of short-term polarity fluctuations in the geomagnetic field? New results from middle to late Miocene sediments of the North Atlantic (DSDP Site 608), *Timescales of the paleomagnetic field* (Vol. 145, pp. 161–174). Amsterdam: American Geophysical Union.

Laj, C., & Channell, J. E. T. (2015). Geomagnetic excursions. In G. Schubert (Ed.), *Treatise on geophysics* (Vol. 5, (2nd ed., pp. 343–383). Amsterdam: Elsevier.

Laj, C., Kissel, C., & Roberts, A. P. (2006). Geomagnetic field behavior during the Iceland basin and Laschamp geomagnetic excursions: A simple transition field geometry? *Geochemistry, Geophysics, Geosystems*, *7*, Q03004. https://doi.org/10.1029/2005GC001122

Lanci, L., & Lowrie, W. (1997). Magnetostratigraphic evidence that tiny wiggles in the oceanic magnetic anomaly record represent geomagnetic paleointensity variations. *Earth and Planetary Science Letters*, *148*, 581–592.

Lhuiller, F., Hulot, G., & Gallet, Y. (2013). Statistical properties of reversals and chrons in numerical dynamos and implications for the geodynamo. *Physics of Earth and Planetary Interiors*, *220*, 19–36. https://doi.org/10.1016/j.pepi.2013.05.005

Lowrie, W., & Kent, D. V. (2004). Geomagnetic polarity time scale and reversal frequency regimes, *Timescales of the paleomagnetic field* (Vol. 145, pp. 117–129). Amsterdam: American Geophysical Union.

Meduri, D. G., & Wicht, J. (2016). A simple stochastic model for dipole moment fluctuations in numerical dynamo simulations. *Frontiers in Earth Science*, *22*, UNSP 38. https://doi.org/10.3389/feart.2016.00038

Merrill, R. T., & McFadden, P. L. (1994). Geomagnetic field stability: Reversal events and excursions. *Earth and Planetary Science Letters*, *121*, 57–69.

Naidu, P. S. (1971). Statistical structure of geomagnetic field reversals. *Journal of Geophysical Research*, *76*, 2649–2662.

Ogg, J. G. (2012). Geomagnetic polarity time scale. In F. M. Gradstein (Ed.), *The geologic time scale 2012* (pp. 85–113). Amsterdam: Elsevier Science.

Olson, P., Christensen, U. R., & Driscoll, P. E. (2012). From superchrons to secular variation: A broadband dynamo frequency spectrum for the geomagnetic dipole. *Earth and Planetary Science Letters*, *319*, 75–82. https://doi.org/10.1016/j.epsl.2011.12.008

Quidelleur, X., Gillot, P. Y., Carlut, J., & Courtillot, V. (1999). Link between excursions and paleointensity inferred from abnormal field directions recorded at La Palma around 600 ka. *Earth and Planetary Scence Letters*, *168*, 233–242.

Risken, H. (1989). *The Fokker-Planck equation*. New York: Springer.

Roberts, A. P., & Lewin-Harris, J. C. (2000). Marine magnetic anomalies: Evidence that tiny wiggles represent short-period geomagnetic polarity intervals. *Earth and Planetary Science Letters*, *183*, 375–388.

Schaeffer, N., Jault, D., Nataf, H.-C., & Fournier, A. (2017). Turbulent geodynamo simulations: A leap towards Earth's core. *Geophysical Journal International*, *211*, 1–29. https://doi.org/10.1093/gji/ggx265

Scullard, C. R., & Buffett, B. A. (2018). Probabilistic structure of the geodynamo. *Physical Review E*, *98*, 063112.

Tauxe, L. (2006). Long-term trends in paleointensity: The contribution of DSDP/ODP submarine basaltic glass collections. *Physics of Earth and Planetary Interiors*, *156*, 223–241. https://doi.org/1-.1016/j.pepi.2005.03.022

Valet, J. P., Fournier, A., Courtillot, V., & Herrero-Bevera, E. (2012). Dynamical similarity of geomagnetic field reversals. *Nature*, *490*, 89–93.

Valet, J. P., & Plenier, G. (2008). Simulations of a time-varying non-dipole field during geomagnetic reversals and excursions. *Physics of Earth and Planetary Interior*, *169*, 178–193.

Ziegler, L. B., Constable, C. G., Johnson, C. L., & Tauxe, L. (2011). PADM2M: A penalized maximum likelihood model for the 0-2 Ma paleomagnetic axial dipole moment. *Geophysical Journal International*, *184*, 1069–1089.